Hindawi
International Journal of Chemical Engineering
Volume 2019, Article ID 5413960, 8 pages
https://doi.org/10.1155/2019/5413960

Research Article

Immobilization of Lead and Nickel Ions from Polluted Yam Peels Biomass Using Cement-Based Solidification/Stabilization Technique

Ángel Villabona-Ortiz,[1] Candelaria Tejada-Tovar,[1] Ángel Gonzalez-Delgado,[2] Adriana Herrera-Barros,[2] and Gina Cantillo-Arroyo[1]

[1]*Process Design and Biomass Utilization Research Group (IDAB), Chemical Engineering Department, University of Cartagena, Cartagena de Indias 130015, Colombia*
[2]*Nanomaterials and Computer Aided Process Engineering Research Group (NIPAC), Chemical Engineering Department, University of Cartagena, Cartagena de Indias 130015, Colombia*

Correspondence should be addressed to Ángel Gonzalez-Delgado; agonzalezd1@unicartagena.edu.co

Received 14 November 2018; Revised 5 February 2019; Accepted 13 February 2019; Published 10 March 2019

Academic Editor: Sébastien Déon

Nowadays, biomass has been employed to prepare biosorbents for heavy metals uptake; however, further disposal of polluted material has limited its application. In this work, nickel and lead removal was performed using yam peels and the resulting polluted biomass was mixed with concrete to produce bricks. The biomass was characterized by FT-IR analysis for testing functional groups diversification before and after adsorption process. The effect of adsorbent dosage, temperature, and initial solution concentration was evaluated to select suitable values of these parameters. Adsorption results were adjusted to kinetic and isotherm models to determine adsorption mechanism. Desorption experiments were also performed to determine the appropriate desorbing agent as well as its concentration. Immobilization technique of cement-based solidification/stabilization was applied and the polluted biomass was incorporated to concrete bricks at 5 and 10%. Mechanical resistance and leaching tests were carried out to analyze the suitability of heavy metals immobilization. The suitable values for dosage, temperature, and initial solution concentration were 0.5 g/L, 40°C and 100 ppm, respectively. The kinetic model that best fitted experimental results was pseudo-second order indicating a dominant physicochemical interaction between the two phases. The highest desorption yields were found in 52.47 and 74.84% for nickel and lead ions. The concrete bricks exhibited compression resistance above 5 MPa and all the leachate reported concentrations below the environmental limit. These results suggested that nickel and lead immobilization using concrete bricks is a good alternative to meet disposal problems of contaminated biomass.

1. Introduction

The water sources have been deteriorated in the last decades because of the anthropogenic activities discharging pollutants into the environment. Toxic heavy metals such as nickel and lead are one of the most perilous pollutants due to their toxicity and persistence [1]. These contaminants have become focus of attention due to their acute and chronic effects on plants and animals [2]. Nickel ions in groundwater can be attributed to mining, smelting, metal plating, or metal recycling facilities [3]. Lead is found in activities involving smelting, combustion of leaded gasoline, and fertilizers [4]. The effects of these pollutants on public health and environment have motivated the development of new environment friendly [5].

Adsorption process appears to be a good alternative for water treatment due to its several advantages as convenience, ease operation, and simplicity [6]. Several materials provided by agricultural industry have been tested as biosorbents because of their cost-effectiveness and availability [7]. Some of these are wastes from fruit and vegetable processing industries (pineapple, citrus, banana, and mango peels) or

root tubers as yam and cassava peels [8]. However, the disposal of polluted biomass after sorption-desorption cycles seems to be a limitation for adsorption application. To face this problem, immobilization is an effective alternative to reduce the potential migration of heavy metals by changing the physical and chemical properties of the wastes [9]. One of the immobilization methods is the cement-based solidification/stabilization [10]. In this work, adsorption of nickel and lead was studied using yam peels biomass and cement-based immobilization method was implemented for polluted biomass disposal.

2. Materials and Methods

2.1. Biosorbent Preparation. The yam peels were collected from local markets and washed with water to remove surface adhered particles that can affect adsorption process. This biomass was dried and grounded to achieve particle size of 1 mm [11]. The resulting material was characterized by Fourier-Transform Infrared Spectroscopy (FT-IR) in order to determine main functional groups on biomass surface.

2.2. Adsorption Tests. Stock solutions of nickel and lead were prepared by adding 1.598 g and 4.479 g of Pb $(NO_3)_2$ and Ni $(NO_3)_2$, respectively, into 1000 mL of deionized water. The optimum solution pH to conduct the experiments was selected by analyzing the effect of pH variations (2, 4, and 6) on removal yield. Stirring speed is a key parameter in adsorption process; however, previous work of authors suggested a value of 200 rpm [12]. The operating conditions for further adsorption tests were selected for nickel and the results were also considered for lead. The effect of adsorbent dosage was evaluated by varying this parameter between 0.1 and 1 g/L. The initial solution concentration as well as temperature was varied to determine its suitable values. The adsorption experiments were performed in a batch reactor, and the remaining heavy metal concentration was calculated using an atomic absorption spectrophotometer [13].

2.3. Adsorption Isotherm and Kinetics. The experimental data are adjusted to the following kinetic models: pseudo-first order, pseudo-second order, intraparticle diffusion, and Elovich. Regarding isotherms, the selected models were Langmuir and Freundlich. The sum of square represents the judge-parameter to find out if the model fits well the data. The aim of fitting these equations is to obtain additional information about the fundamental interactions between the metal ions and the biosorbent as charged surface [14]. Tables 1 and 2 shows the governing equations employed to determine both kinetic and isotherm parameters.

2.4. Sorption-Desorption Cycles. After adsorption process, the biomass was filtered and weighted. Two types of desorbing agents (hydrochloric and nitric acids) were used in order to select which of them allows to obtain the highest desorption yield. These tests were performed in batch mode at 25°C and 180 rpm during 3 hours. Desorption yield was calculated using an atomic absorption spectrophotometer. Then, biomass was regenerated using 1 M calcium chloride under a temperature of 4°C. The biosorbent was filtered, dried, and used for the second adsorption cycle as reported by Mata et al. [15] The desorbing agent concentration was also evaluated by varying this parameter in 0.1, 0.5, and 1 M.

2.5. Polluted Biomass Immobilization. The biomass immobilization requires the preparation of a concrete matrix, which is based on 18.1% of cement, 30.6% of sands, 43.2% of grit, and 8.1% of water [16]. This matrix was modified by adding polluted biomass (5 and 10%). The resulting material was used to produce bricks of 5 cm × 5 cm × 5 cm after hardening them for 28 days.

2.6. Mechanical Resistance Testing. The compression resistance of the concrete was tested after biomass immobilization using a digital universal testing machine TINIUS OLSEN, which provides an axial force to concrete bricks until failure.

2.7. Leaching Tests. These tests were based on the methodology described by Ukwatta and Mohajerani [17]. A sample of the solid was collected and mixed with water for 5 minutes. The pH was adjusted by adding 1 M HCl solution. The mixture was heated at 50°C for 10 minutes and cooled to measure the pH confirming it was below 5.

3. Results and Discussion

3.1. Biomass Characterization. As shown in Figure 1, the yam peels biomass exhibited an absorption band around 3005 and 1050 cm^{-1} attributed to hydroxyl stretching vibrations. The peaks at 3400 and 1450 cm^{-1} correspond to carboxylic acid group. The stretching vibrations of C-H group in alkenes were identified at 2920 cm^{-1}. Herrera-Barros et al. [18] pointed out that the peak at 1732 cm^{-1} is assigned to C=O carbonyl group. After nickel and lead uptake, it was observed relevant variations in biosorbent spectrum, especially in the adsorption bands intensity. The peak at 3400 cm^{-1} moved towards 3300 cm^{-1} because of the stretching of hydroxyl group. The spectrum of YP-Pb(II) showed a disappearance of the peak corresponding to the carboxylic acids at 2360 cm^{-1}. For YP-Ni(II) spectrum, it was identified the presence of C=C functional group around 1400 cm^{-1}, which confirms the interaction of hydroxyl and carboxyl groups during adsorption process of nickel and lead onto yam peels biomass.

3.2. Adsorption Batch Experiments

3.2.1. Effect of Solution pH. The solution pH substantially affects the mechanism of metals uptake and should be considered during any adsorption study [7]. Figure 2 depicts the effect of solution pH on the adsorption performance of

Table 1: Mathematical expressions of kinetic models.

Kinetic model	Equation	Parameters
Pseudo-first order	$q_t = q_e(1 - e^{-kt})$	q_e, adsorption capacity at equilibrium (mg/g) k_1, pseudo-1st order constant (min^{-1})
Pseudo-second order	$q_t = t/((1/(k_2 q_e^2)) + (t/q_e))$	k_2 pseudo-2nd order constant (g/mg·min) q_e, adsorption capacity at equilibrium (mg/g)
Elovich	$q_t = (1/\beta)\ln(\alpha\beta) + (1/\beta)\ln t$	α, Elovich constant (mg/g min) β, Elovich exponent (g/mg)
Intraparticle diffusion	$q_t = k\sqrt{t}$	k, diffusion constant

Table 2: Parameters of isotherm models.

Isotherm	Equation	Parameters
Freundlich	$q_e = K_F C_e^{1/n}$	K_F, indicator of the absorption capacity (mg/g) $1/n$, heterogeneity factor C_e, concentration of the metal (mg/L)
Langmuir	$q_e = (q_{max} b C_e)/(1 + bC_e)$	q_{max}, maximum quantity of the metal/mass of biomass (mg/g) b, affinity of union sites C_e concentration of the metal (L/mg)

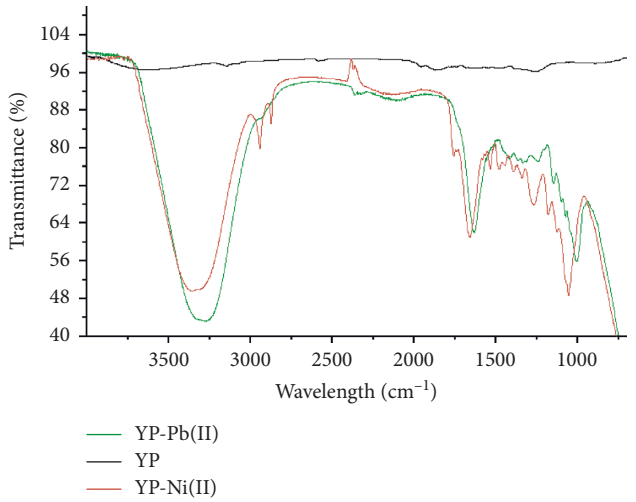

Figure 1: FT-IR spectrum of yam peels biosorbent before and after adsorption of nickel and lead.

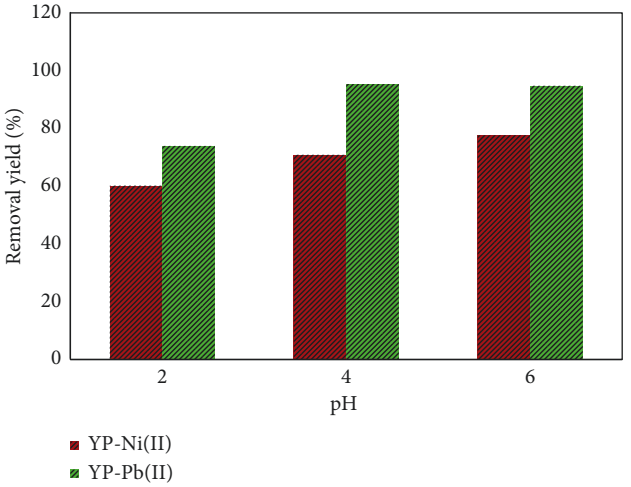

Figure 2: Influence of solution pH on yam peels removal yield.

yam peels. The acid conditions reduce the removal yields attributed to ionic charge of the heavy metal ions solution. The adsorption of both metals were favored at elevated pH because of the deprotonation of functional groups that serve as binding sites; therefore, nickel and lead ions can access easily to these sites [19]. The removal yields results were higher for lead than those for nickel ions, which could be assigned to a higher electrostatic attraction between the negative charge on the biomass and these positive metal cations.

3.2.2. Effect of Biosorbent Dosage. Figure 3 shows the influence of biosorbent dosage on adsorption process using yam peels for nickel uptake. It was found that the highest adsorption capacity (6.14 mg/g) was achieved using a dosage of 0.5 g/L. The adsorption capacity increased with further

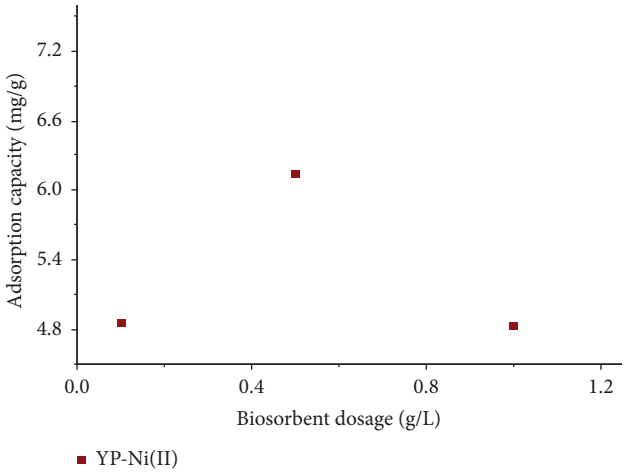

Figure 3: Effect of biosorbent dosage on adsorption capacity for nickel uptake.

increases in the biosorbent amount [20]. However, it starts to decrease because of the formation of biomass agglomerates [21]. In addition, stearic, conformational, or other defenses may be present affecting the heavy metal uptake [22].

3.2.3. Effect of Temperature and Solution Concentration. Table 3 summarizes the adsorption results by varying temperature and initial solution concentration for nickel uptake onto yam peels biomass. It was found that the highest adsorption capacity was achieved at 33.78°C and 200 ppm. However, the suitable conditions for further experiments were 40°C and 100 ppm because of the similar results using less pollutants amount.

3.2.4. Continuous Adsorption Experiments. Continuous adsorption experiments were conducted in order to analyze the effect of adsorption cycles on adsorption capacity. Figure 4 shows a gradual reduction on adsorption capacity as increases the number of cycles. For nickel uptake, it was found a slight variation in adsorption capacity for the three cycles. Lead reported significant changes in this variable. In the first two cycles, higher amount of lead was adsorbed in comparison to nickel; however, the adsorption capacity decreased below nickel results in the third cycle. The differences between both heavy metals uptake informs about a higher adsorption onto yam peels biomass surface attributed to the higher electrons valence number or ionic radius of lead [23]. The ionic radius of lead and nickel are 1.2 and 0.78, respectively, which confirms the results shown in this work.

3.3. Adsorption Kinetics and Isotherms. Adsorption experiments were also carried out to determine parameter values of the selected kinetic models (pseudo-first order, pseudo-second order, Elovich, and intraparticle diffusion). The sum of square (SS) provides information about the well-fitting of the model, so the minimum SS was identified for YP-Ni(II) and YP-Pb(II). Table 4 lists the kinetic parameters for both metal ions uptake onto yam peels. The minimum SS was reached by the second-order model indicating that the removal from a solution is due to the physicochemical interactions between the two phases (liquid-solid) limited by the chemisorption occurring on the surface. The importance of performing a kinetic modeling leads to estimate the adsorption rates as well as identify possible reaction mechanism [24].

The isotherm model parameters are summarized in Table 5, reporting that the minimum sum of square was reached by Freundlich model for nickel ions and Langmuir model for lead ions; however, the difference between both models for lead ions could be negligible. The fact that nickel ions uptake onto yam peels obeys Freundlich model indicated a biosorbent heterogeneous surface, multilayer formation and non-uniform distribution of heat of adsorption over the surface [25]. On the other hand, Langmuir model is focused on homogenous surface and adsorption process takes place on specific sites that are available just for one molecule of sorbate [26]. This model offers accurate analysis of chemisorption process during heavy metal uptake [27].

Table 3: Influence of temperature and initial concentration on nickel uptake.

Temperature (°C)	Initial concentration (ppm)	Final concentration (ppm)	Adsorption capacity (mg/g)
55	58.57	35.257	4.66
55	341.42	307.212	6.84
55	200	180.250	3.95
70	100	80.644	3.87
70	300	288.234	2.35
40	100	66.678	6.70
40	300	264.143	7.17
76.21	200	169.523	6.09
33.78	200	160.445	7.91
55	58.57	35.257	4.66

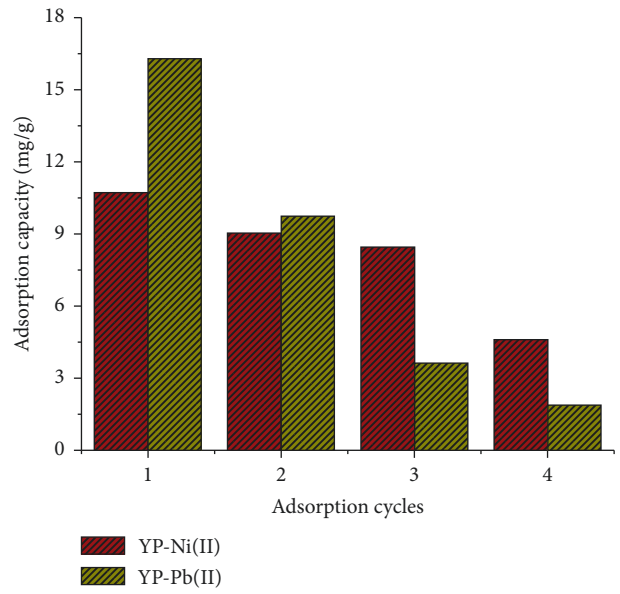

Figure 4: Adsorption capacity of nickel and lead onto yam peels biomass over adsorption cycles.

Table 4: Fitting data of heavy metals adsorption onto yam peels according to kinetic models.

Kinetic model	Parameter	YP-Ni(II)	YP-Pb(II)
Pseudo-first order	$q_{e,1}$ (mg/g)	13.18	19.82
	k_1 (min^{-1})	0.264	1.53
	SS	1.055	0.40
Pseudo-second order	k_2 (g/mg · min)	0.077	0.13
	$q_{e,2}$ (mg/g)	13.32	19.97
	SS	0.735	0.01
Elovich	β (g · min /mg)	3.719	11.78
	α (mg/g)	$4.126E+18$	$2.47E+98$
	SS	0.805	0.15
Intraparticle diffusion	k_3	1.012	1.58
	SS	220.17	491.75

Table 5: Isotherm models for nickel and lead adsorption onto yam peels.

Model	Parameter	YP-Ni(II)	YP-Pb(II)
Langmuir	q_{max} (mg/g)	68.14	98.36
	b (1/mg)	0.0058	0.16
	SS	14.74	3.69
Freundlich	k_f (mg/g)	0.0876	13.42
	$1/n$	1.415	0.86
	SS	8.017	3.70

3.4. Desorption Experiments

3.4.1. Effect of Desorbing Agent Type. The desorbing agent plays an important role in desorption process; hence, nitric and hydrochloric acids were employed for performing desorption experiments. Results revealed that nitric acid exhibited the highest desorption yield (52.47%) for nickel ions. For lead ions, the best result (74.84%) was achieved using hydrochloric acid as shown in Figure 5. The desorption capacity of desorbing agents as both nitric and hydrochloric acids can be attributed to heavy metal ions displacement assigned to the high amount of hydrogen ion found in the acid solution [28].

3.4.2. Effect of Desorbing Agent Concentration. After selecting the desorbing agent type for each heavy metal, it was determined the suitable concentration for performing desorption cycles. Figure 6 shows the effect of nitric acid concentration on desorption yield for nickel ions. It was found that the highest desorption yield of 52.47% was achieved using 0.1 M solution. Similar results were obtained for lead ions (0.1 M solution of hydrochloric acid) reporting a maximum desorption yield of 74.84% as shown in Figure 7. At higher desorbing agent concentration, the biosorbent can be damaged generating a reduction in adsorption and desorption yield. Ngo et al. [29] varied acid concentration between 0.01 and 0.1 M reporting good results using 0.1 M for cadmium, copper, lead, and zinc desorption.

3.4.3. Desorption Cycles. Desorption experiments were performed in four cycles by contacting yam peels biomass with the acid solution. As shown in Figure 8, better results were obtained for Pb(II) ions in comparison to Ni(II). In the first cycle, nickel ions reported higher yield (41.38%), which decreased significantly over desorption cycles. For lead, the highest desorption yield of 74.84% was also reached in the first cycle. Many heavy metal ions cannot be recovered by desorption because of ions keep inside porous structure of adsorbent and are not easy to release [29].

3.5. Mechanical Resistance Testing for Bricks of Yam Peels.

The mechanical compression testing of concrete bricks, which were used for immobilization technique and modified by adding 5 and 10% of yam, peels residual biomass after heavy metals uptake. As shown in Figure 9, mechanical resistance of concrete and biomass contaminated with lead (5 and 10%) exhibited values above 5 MPa, which is the standard limit value. However, the biomass contaminated with nickel

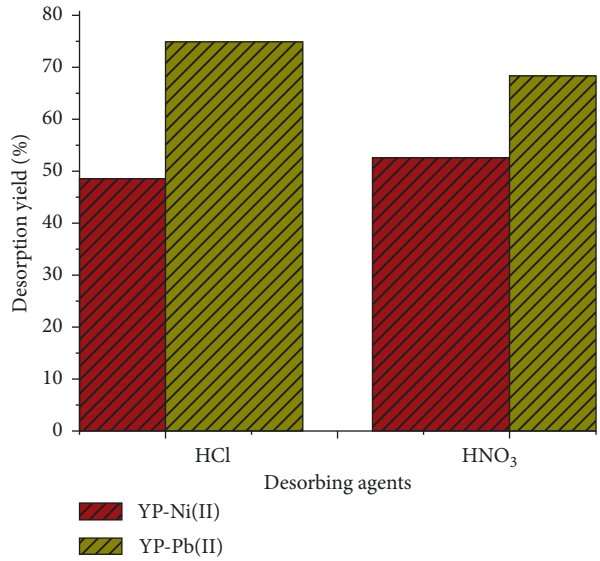

Figure 5: Effect of desorbing agent on desorption process.

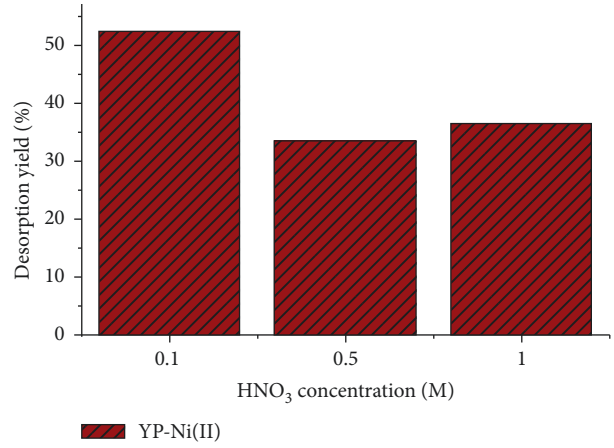

Figure 6: Effect of nitric acid concentration on desorption yield.

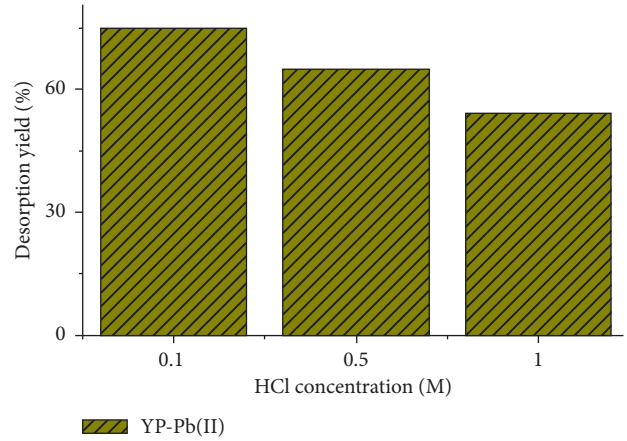

Figure 7: Effect of hydrochloric acid concentration on desorption yield.

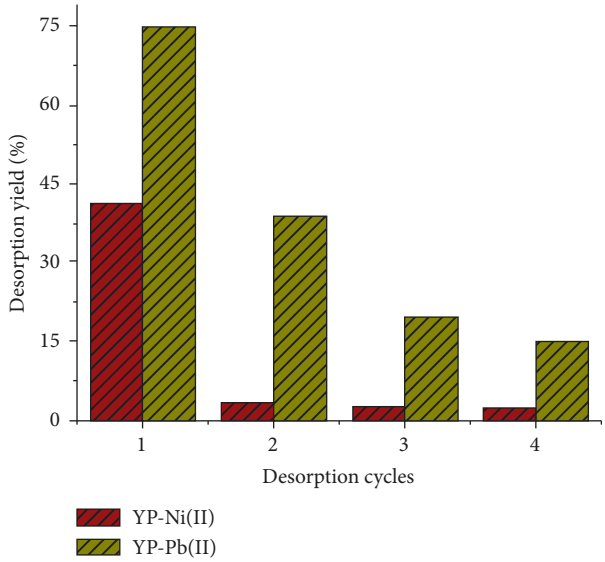

Figure 8: Desorption yield of nickel and lead onto yam peels biomass over cycles.

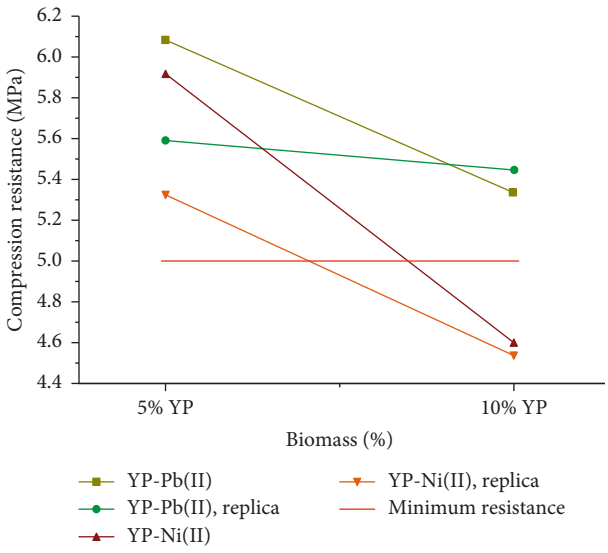

Figure 9: Mechanical compression resistance of concrete bricks with polluted biomass.

reported a single value above this. The highest resistance of 6.1 MPa was reached using 5% yam peel biomass polluted with lead. Similar results were reported by Akyıldız et al. [30], who evaluated the mechanical compression of concrete bricks modified with medical wastes incineration ashes.

3.6. Leaching Tests for Bricks of Yam Peels. The leaching tests were carried out using acetic acid solution and the amount of leached heavy metal ions was calculated by atomic adsorption. Table 6 summarizes the results for all leachate and are compared with the national environmental policy (Decree No. 1594/1984). For lead and nickel, the leached was limited by 0.5 and 2 ppm, respectively. As shown in Figure 10, nickel exhibited higher leached concentration than

Table 6: Leaching test results.

Brick composition	Leachate (ppm)	Environmental policy
5% YP-Pb(II)	0.082	0.5
10% YP-Pb(II)	0.145	0.5
5% YP-Pb(II), replica	0.054	0.5
10% YP-Pb(II), replica	0.155	0.5
5% YP-Ni(II)	0.201	2
10% YP-Ni(II)	0.268	2
5% YP-Ni(II), replica	0.241	2
10% YP-Ni(II), replica	0.307	2

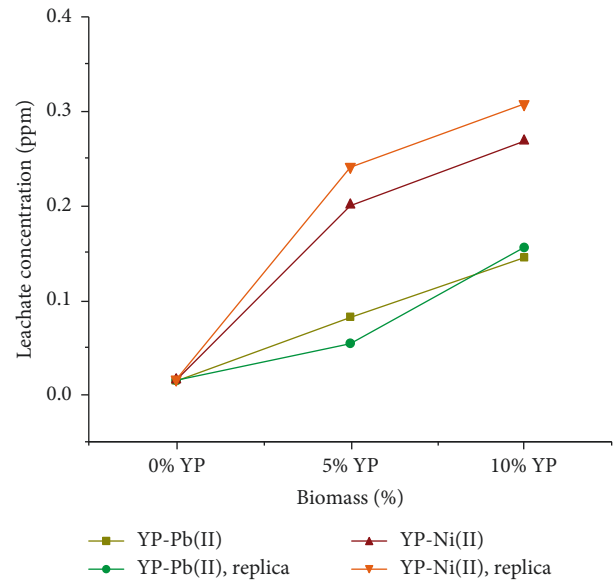

Figure 10: Leaching tests for bricks of yam peels.

lead; however, the leachate for both heavy metals obeyed environmental policy.

The immobilization of heavy metal ions inside the concrete matrix is explained by the physical encapsulation mechanism and chemical bonds as Al-O o Si-O that are found in the concrete, which allows to obtain less leached concentration [31]. In comparison to other works, the encapsulation process in concrete matrix for immobilizing heavy metals results to be a good alternative to solve disposal problems of polluted biomass after adsorption process [30, 32].

4. Conclusions

This work attempted to study the adsorption process of nickel and lead from aqueous solution using yam peels biomass as biosorbent. The yam peels spectrum exhibited the presence of hydroxyl and carboxyl groups, which enhance adsorption process. This spectrum varied significantly after Ni(II) and Pb(II) ions uptake confirming the retention of these pollutants onto biomass surface. Suitable conditions for performing further experiments were selected as 0.5 g/L of dosage, 40°C of temperature, and 100 ppm of initial solution concentration. The pH of the solution presents a direct effect on removal performance for both heavy metal

ions, and pH = 6 reports the maximum adsorption yields. The pseudo-second order and Freundlich models best fitted both adsorption kinetics and isotherm. For desorption experiments, the nitric and hydrochloric acids were selected for nickel and lead ions with desorption yields of 52.47 and 74.84%, respectively. The optimal desorbing agent concentration was found to be 0.1 M. The polluted biomass was used to prepare concrete bricks reporting compression resistance above 5 MPa. The leaching test indicated that this alternative for solving disposal obeyed environmental policy for leachate.

Data Availability

Previously reported research articles' data were used to support this study and are available at Sciencedirect. These prior studies (and datasets) are cited at relevant places within the text as references.

Conflicts of Interest

The authors declare that there are no conflicts of interest regarding the publication of this paper.

Acknowledgments

Authors express their gratitude to University of Cartagena for providing the reagents and equipment required to perform this work.

References

[1] M. Cui, Y. Lee, J. Choi et al., "Evaluation of stabilizing materials for immobilization of toxic heavy metals in contaminated agricultural soils in China," *Journal of Cleaner Production*, vol. 193, pp. 748–758, 2018.

[2] A. Das and J. W. Osborne, "Enhanced lead uptake by an association of plant and earthworm bioaugmented with bacteria," *Pedosphere*, vol. 28, no. 2, pp. 311–322, 2018.

[3] R. T. Wilkin and D. G. Beak, "Uptake of nickel by synthetic mackinawite," *Chemical Geology*, vol. 462, pp. 15–29, 2017.

[4] F. Cai, X. Wu, H. Zhang et al., "Impact of TiO_2 nanoparticles on lead uptake and bioaccumulation in rice (*Oryza sativa* L.)," *NanoImpact*, vol. 5, pp. 101–108, 2017.

[5] J. Li, G. Yu, S. Xie et al., "Immobilization of heavy metals in ceramsite produced from sewage sludge biochar," *Science of the Total Environment*, vol. 628-629, pp. 131–140, 2018.

[6] A. Bhatnagar, M. Sillanpää, and A. Witek-Krowiak, "Agricultural waste peels as versatile biomass for water purification—a review," *Chemical Engineering Journal*, vol. 270, pp. 244–271, 2015.

[7] A. Herrera-Barros, C. Tejada-Tovar, T. Villabona-Ortiz et al., "Effect of pH and particle size for lead and nickel uptake from aqueous solution using cassava (*Manihot esculenta*) and yam (*Dioscorea alata*) residual biomasses modified with titanium dioxide nanoparticles," *Indian Journal of Science and Technology*, vol. 11, no. 21, pp. 1–7, 2018.

[8] T. E. Aruna, O. C. Aworh, A. O. Raji, and A. I. Olagunju, "Protein enrichment of yam peels by fermentation with *Saccharomyces cerevisiae* (BY4743)," *Annals of Agricultural Sciences*, vol. 62, no. 1, pp. 33–37, 2017.

[9] B. Guo, B. Liu, J. Yang, and S. Zhang, "The mechanisms of heavy metal immobilization by cementitious material treatments and thermal treatments: a review," *Journal of Environmental Management*, vol. 193, pp. 410–422, 2017.

[10] M. Vyšvaril and P. Bayer, "Immobilization of heavy metals in natural zeolite-blended cement pastes," *Procedia Engineering*, vol. 151, pp. 162–169, 2016.

[11] A. Herrera-Barros, C. Tejada-Tovar, Á. Villabona-Ortíz, Á. González-Delgado, and A. Reyes-Ramos, "Adsorption study of Ni(II) and Pb(II) onto low-cost agricultural biomasses chemically modified with TiO_2 nanoparticles," *Indian Journal of Science and Technology*, vol. 11, no. 21, pp. 1–9, 2018.

[12] C. Tejada-Tovar, Á Villabona-Ortiz, and E. Ruiz-Paternina, "Adsorción de Ni(II) por cáscaras de ñame (*Dioscorea rotundata*) y bagazo de palma (*Elaeis guineensis*) pretratadas," *Luna Azul*, vol. 42, pp. 30–43, 2016.

[13] C. Tejada-Tovar, A. Herrera, and J. Núñez, "Adsorción competitiva de Ni(II) y Pb(II) sobre materiales residuales lignocelulósicos," *Investigaciones Andina*, vol. 17, pp. 1355–1367, 2015.

[14] M. Soleimani and Z. H. Siahpoosh, "Determination of Cu(II) in water and food samples by Na^+ cloisite nanoclay as a new adsorbent: equilibrium, kinetic and thermodynamic studies," *Journal of the Taiwan Institute of Chemical Engineers*, vol. 59, pp. 413–423, 2015.

[15] Y. N. Mata, M. L. Blázquez, A. Ballester, F. González, and J. A. Muñoz, "Studies on sorption, desorption, regeneration and reuse of sugar-beet pectin gels for heavy metal removal," *Journal of Hazardous Materials*, vol. 178, no. 1–3, pp. 243–248, 2010.

[16] R. A. Lara-Díaz and R. M. Melgoza-Alemán, "Solidificación-estabilización de cromo, níquel y plomo en una matriz sólida de hormigón fabricada con cemento Portland," *Información Tecnológica*, vol. 20, pp. 29–38, 2009.

[17] P. Ukwatta and A. Mohajerani, "Effect of organic content in biosolids on the properties of fired-clay bricks incorporated with biosolids," *Journal of Materials in Civil Engineering*, vol. 29, no. 7, article 04017047, 2017.

[18] A. Herrera-Barros, C. Tejada-Tovar, and E. Ruiz-Paternina, "Utilización de biosorbentes para la remoción de níquel y plomo en sistemas binarios," *Revista Ciencia en Desarrollo*, vol. 7, pp. 31–36, 2016.

[19] M. Basu, A. K. Guha, and L. Ray, "Adsorption of lead on cucumber peel," *Journal of Cleaner Production*, vol. 151, pp. 603–615, 2017.

[20] C. Sakulthaew, C. Chokejaroenrat, A. Poapolathep, T. Satapanajaru, and S. Poapolathep, "Hexavalent chromium adsorption from aqueous solution using carbon nano-onions (CNOs)," *Chemosphere*, vol. 184, pp. 1168–1174, 2017.

[21] L. Prasanna, J. Yang, Y. Chang et al., "Low-cost magnetized *Lonicera japonica* flower biomass for the sorption removal of heavy metals," *Hydrometallurgy*, vol. 165, pp. 81–89, 2016.

[22] A. R. Albis, L. V. Cajar R, and M. I. Domínguez, "Análisis cinético de la adsorción de Cr (VI) en soluciones acuosas a concentraciones de 10-20 mg/L con el uso de cáscara de yuca amarga (*Manihot esculenta*)," *Prospectiva*, vol. 13, no. 2, pp. 64–71, 2015.

[23] L. Cardero and L. Garcell, "Efecto del potencial iónico sobre la adsorción específica de cationes en suspensiones de laterita y de cieno carbonatado," *Tecnología Química*, vol. 30, pp. 78–86, 2010.

[24] D. Robati, "Pseudo-second-order kinetic equations for modeling adsorption systems for removal of lead ions using

multi-walled carbon nanotube," *Journal of Nanostructure in Chemistry*, vol. 3, p. 55, 2013.

[25] C. Tejada-Tovar, A. Herrera-Barros, Á. Villabona-Ortíz, Á. González-Delgado, and J. Núñez-Zarur, "Hexavalent chromium adsorption from aqueous solution using orange peel modified with calcium chloride: equilibrium and kinetics study," *Indian Journal of Science and Technology*, vol. 11, no. 17, pp. 1–10, 2018.

[26] D. D. Duong, *Adsorption Analysis: Equilibria and Kinetics,* vol. 2, Imperial College Press, London, UK, 1998.

[27] J. P. Vareda, A. J. M. Valente, and L. Durães, "Heavy metals in Iberian soils: removal by current adsorbents/amendments and prospective for aerogels," *Advances in Colloid and Interface Science*, vol. 237, pp. 28–42, 2016.

[28] D. Guzmán and N. Elizabeth, "Caracterización del proceso de biosorción de metales pesados mediante residuos sólidos de café," Doctorado thesis, Universidad Autónoma de Nuevo León, San Nicolás de los Garza, Mexico, 2012.

[29] H. Ngo, A. Abdolali, G. Wenshan et al., "Characterization of a multi-metal binding biosorbent: chemical modification and desorption studies," *Bioresource Technology*, vol. 193, pp. 477–487, 2015.

[30] A. Akyıldız, E. Tinmaz, and A. Yildiz, "Compressive strength and heavy metal leaching of concrete containing medical waste incineration ash," *Construction and Building Materials*, vol. 138, pp. 326–332, 2017.

[31] W. Gwenzi and N. M. Mupatsi, "Evaluation of heavy metal leaching from coal ash-versus conventional concrete monoliths and debris," *Waste Management*, vol. 49, pp. 114–123, 2016.

[32] P. Hartwich and A. Vollpracht, "Influence of leachate composition on the leaching behaviour of concrete," *Cement and Concrete Research*, vol. 100, pp. 423–434, 2017.